CORRELATING STRUCTURE AND FUNCTION - *IN SITU* X-RAY ANALYSIS OF HIGH QE ALKALI-ANTIMONIDE PHOTOCATHODES

J. Smedley, K. Attenkofer and S. Schubert
Brookhaven National Laboratory, Upton, NY 11973, USA
T. Vecchione, J. Wong, T. Forrest and H. A. Padmore
Lawrence Berkeley National Laboratory, Berkeley, CA 94720, USA
E. M. Muller, X. Liang, M. Ruiz Oses and I. Ben-Zvi
Stony Brook University, Stony Brook, NY 11794, USA
J. Xie, Argonne National Laboratory, Lemont, IL 60439, USA

Abstract

Alkali antimonide photocathodes have high quantum efficiency and low emittance when illuminated by visible light, and are thought to be well suited for use in high-brightness photoinjectors for 4th generation light sources. Here we report on the growth of multi-alkali K_2CsSb cathodes on [100] silicon substrates measured using *in situ* x-ray scattering. Correlations between cathode structure, growth parameters and the resulting quantum efficiency (QE) are also explored. The best cathodes in this study have a QE at 532 nm in excess of 6% and are structurally textured K_2CsSb with grain sizes in excess of 20 nm. In an attempt to reduce the complexity of the current growth methodology, we are also making alkali antimonides in parallel via the reaction of bulk materials in an inert environment. This approach has the advantage that the desired stoichiometry can be obtained exactly. Initial diffraction results from prepared bulk materials are promising and show the formation of well reacted K_3Sb. In the future, we intend to transfer this material to smooth thin photocathode films by either sputtering or pulsed laser deposition.

INTRODUCTION

Alkali Antimonides have been recently proven to have excellent characteristics as low emittance, high quantum efficiency photocathodes. They offer reasonably robust operation in ultra-high vacuum photoguns, such as DC or VHF designs [1-3]. Several issues remain in the growth and development of these materials for accelerator applications. The surface roughness has been shown to be a problem [4], causing a strong dependence of the intrinsic emittance on the applied field. Further, the reproducibility of growth and the lifetime in high average current operation remain challenges. Much of the early development of this material was motivated by applications in photo-detectors such as image intensifiers and photo-multiplier tubes (PMT); these devices have different requirements, different substrates and different growth environments.

The current work focuses on understanding the formation of these materials, both structurally and chemically, with the goal of altering the growth to produce cathodes with less roughness, better stoichiometry, and larger crystal grains. The tools being used are *in situ* x-ray diffraction (XRD), grazing incidence small angle x-ray scattering (GISAXS) and x-ray reflection (XRR). These tools enable determination of the crystal form of the cathode at each phase of growth, the film thickness and roughness, the texture and grain size of the film, and the presence of “imperfectly reacted” material. This work has been carried out at the National Synchrotron Light Source (NSLS) using beamline X21 and at the Cornell High Energy Synchrotron Source (CHESS) using beamline G3.

EXPERIMENT

The cathodes are grown in an ultra-high vacuum chamber, with a typical operating pressure of 0.2 nTorr. Residual gas analysis confirms that the partial pressures of reactive gasses (H_2O, CO) are better than 0.05 nTorr. The chamber has Be windows to allow x-ray irradiation of the sample during growth and collection of scattered and reflected x-rays via two Pilatus 100K x-ray cameras. One of the cameras is situated in small angle scattering/reflection mode while the other simultaneously records wide angle diffraction data during the deposition.

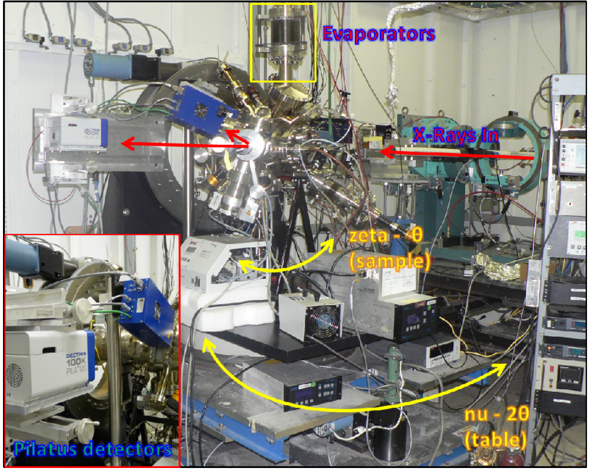

Figure 1: Growth chamber mounted on beamline X21.

The experiments are performed with a photon flux of approximately 2×10^{12} ph/sec with an energy of 10 keV (at NSLS) and 4×10^{13} ph/sec with an energy of 9.8 keV (at CHESS). The incident x-ray beam is typically 1 mm wide and 0.5 mm high. Substrates are electrically isolated; photocurrent is continuously monitored during growth via irradiation with a 5 mW green laser (532 nm) and application of a -10V bias. Deposition rates are monitored using a quartz crystal film thickness monitor (FTM), which is calibrated by flourscent x-ray analysis (EDX) of deposited films. During growth, the x-ray incidence angle is 1.8 degrees (2.5 degrees at CHESS), resulting in an illumined area covering most of the 2 cm substrate width. X-ray movies are acquired during growth, with an exposure time of 20s/ frame (2s/frame at CHESS, due to higher flux). Antimony is evaporated from PtSb beads; alkali-Bi sources from Alvatech are used to supply Potassium and Cesium. Deposition is sequential, with Sb evaporated, then K, then Cs.

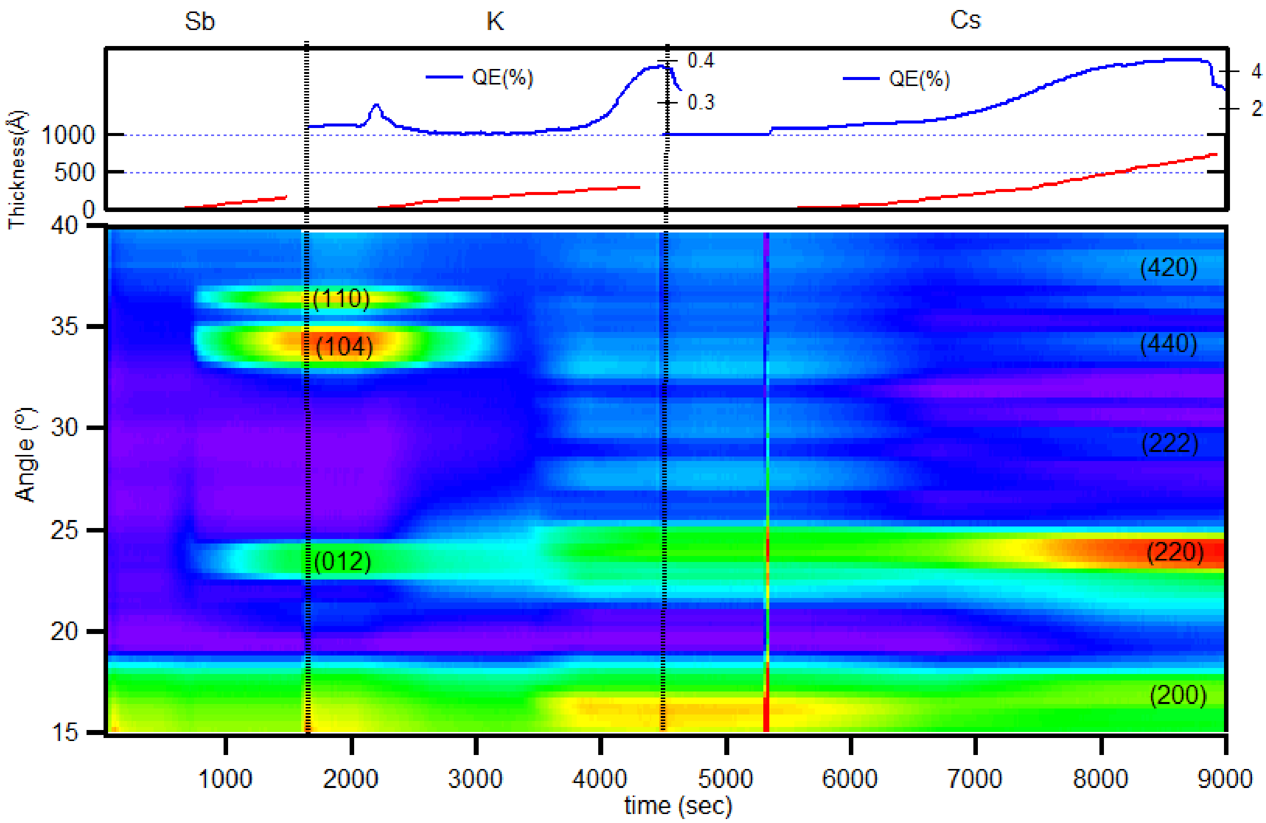

Figure 2: Growth of a cathode on Si [100] with XRD monitoring. The blue line shows the time evolution of the QE at 532 nm (the Sb film has no emission at this wavelength). The red line shows the film thickness measured by the FTM. The 2D image shows the crystal evolution of the cathode. The crystal reflection order of the Sb film and the final K_2CsSb film are labeled on the plot.

RESULTS

Figure 2 shows the data acquired with this system during one cathode growth (of about 12 to date) [5]. The time evolution of the cathode growth demonstrates several significant phases. The Sb film is deposited at 0.2 Å/s, with the substrate temperature at 100 C. The film is amorphous for the first 4 nm of growth (t=700 s), then forms a clear crystal pattern with a [003] surface normal texture. The onset of a crystalline phase occurs far earlier than the 18 nm from the PMT literature [6], likely due to a difference in deposition rate. Note that the plot in fig. 2 shows the in-plane scattering, thus the [003] peak is not observed. The full film thickness is 15 nm, confirmed by XRR and FTM. XRR measurements (not shown) made on similar films yield a roughness of 0.3 nm.

In preparation for potassium deposition, the substrate temperature is increased to 135 C. Potassium is deposited at 0.2 Å/s; initially there is no change in the Sb crystal structure. A small spike is observed in the photoresponse when the deposition begins, presumably due to the reduction of the workfunction of the metallic Sb by the addition of a K surface layer. When the total K deposited reaches 20 nm (t=3000 s), the Sb crystal begins to dissolve. By t=3500 s, K_3Sb crystals have begun to form (but only after the Sb has completely dissolved – there is no gradual change of Sb into K_3Sb, and no crystalline layer of K). The K-Sb film also includes other K_xSb forms. The film at this point is too rough for GISAXS to determine the thickness, however XRR on a similar cathode in this system suggests that the total film thickness is less than the sum of the potassium and antimony film thickness observed on the FTM. The roughness of this film is 0.5 nm RMS with XRR.

For the Cesium deposition, the substrate is held at 135 C. The deposition rate for Cs is also 0.2 Å/s. There is a step rise in the QE when the Cs deposition begins, again likely due to a reduction in the workfunction. The QE then exponentially rises with time; at the same time, the cathode is becoming progressively more fully cubic K_2CsSb. It appears that the Cs catalyzes the formation of much better crystals, as the cathode achieves a much more fully defined texture. The final surface texture is [220].

The final QE is 4.1% for the cathode shown. It is interesting to note that this cathode has a small amount of residual contaminants. There is a correlation between the presence of contaminants and the QE; other cathodes have been grown with QE up to 6.3% at 532 nm – these cathodes lack contaminants to within the resolution of the system, though significant variation in the predominant surface texture has been observed. In vacuum AFM on similar cathodes yields a roughness of 25 nm rms. This is much larger than that expected from XRR. This difference provides insight into the structure of the film – the AFM shows pillars with a sub 100 nm spatial period. These pillars must be approximately the same height to yield the XRR result, but between these pillars, the film has deep fissures.

Scherrer analysis of the XRD peak width suggests that the grain size of films grown in this manner is 15-20 nm, increasing with increasing initial Sb thickness. Larger grains and a smoother surface would likely lead to more uniform emission, and a lower intrinsic emittance.

SYNTHESIS OF BULK K_3SB

One of the main challenges in the synthesis of alkali antimonides is the precise control of stoichiometry and smoothness. In order to control stoichiometry with far greater precision and investigate the effect of doping, we have made K_3Sb using a bulk reaction method. Gram quantities of Sb and K are weighed out in the correct proportion in an O_2 & H_2O free glove box (< 0.1 ppm), then transferred into a quartz tube, which is then evacuated and transferred to an oven. The materials react to form a powder. Post-reaction, the tube is returned to the glove box; a small quantity of power is sealed under mylar and transferred to a powder diffraction system.

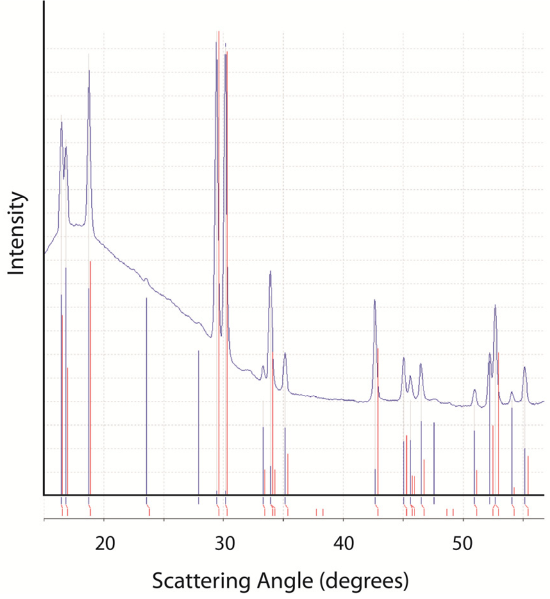

Figure 3: Powder pattern from K_3Sb, reacted at 250 C for 4 hours. (blue: measured intensities, red: calculated intensities).

A typical powder pattern is shown in fig. 3, for a 4 hour reaction at 250 C. The background is caused by the thick mylar which has to be used to seal the powder for diffraction measurements. It can be seen that the measured powder pattern is very close to that expected for single phase K_3Sb. The next stage is to react Cs with K_3Sb, and look at co-reaction of K and Cs with Sb. The great advantage of this method is that it is relatively easy to get fractional % control of the stoichiometry, something that is impossible with the thin film method. Once formed into a target, Pulsed Laser Deposition (PLD), Sputtering or thermal evaporation can be used to deposit a thin film photocathode. All three of these techniques are possible in the deposition system shown in Fig. 1.

CONCLUSIONS

In situ materials analysis tools have the potential to revolutionize our understanding of thin film photocathode growth. Observing formation of the cathodes in real time has led to a significant change in our understanding of how these materials form. The Sb film is crystalline at 4 nm in thickness, with a well defined texture. Before the K_xSb compounds can form, the Sb crystal must fully dissolve – there is no gradual change of Sb into K_3Sb. The Cs step causes a dramatic improvement in the crystalline structure – what was a defect-rich crystal becomes progressively a well-ordered crystal as the Cs diffuses in. This leads us to believe that the primary effect of Cs (beyond lowering the work function) is to stabilize the crystal structure, reducing defect scattering and increasing the electron mean free path (and thereby the QE).

We have investigated one trajectory in a complex space of sample temperature and deposition rate. We will investigate other trajectories, particularly investigating the effect of deposition rate. It may be that the reaction of K with Sb always leads to a rough film due to nucleation of large grains. For this reason we are also investigating the growth of these materials through multilayer and co-deposition strategies. The ultimate aim is to find a method of producing ultra-smooth thin film stoichiometric cathodes with a defined doping.

This work was supported by the Director, Office of Science, Office of Basic Energy Sciences of the U. S. Department of Energy, under Contract No. DE-AC02-05CH11231, DE-AC02-98CH10886, KC0407-ALSJNT-I0013, and DE-SC0005713. Use of CHESS is supported by NSF award DMR-0936384.

REFERENCES

[1] I. Bazarov, et al., Appl. Phys. Lett. 98(22), 224101-3 (2011).
[2] R. R. Mammei, et al., Phys. Rev. ST - Accel. Beams **16**, 033401 (2013).
[3] T. Vecchione, et al., Appl. Phys. Lett. **99,** 034103 (2011).
[4] T. Vecchione, et al., Proceedings of IPAC2012, New Orleans, Louisiana, USA, 655.
[5] M. Ruiz Oses, et al., to be published in Appl. Phys. Lett. Mat.
[6] A.H Sommer, J. of Appl. Phys. **37** , 2789 (1966).